

David G. Richards

N^* Resonances in Lattice QCD from (mostly) Low to (sometimes) High Virtualities

Received: date / Accepted: date

Abstract I present a survey of calculations of the excited N^* spectrum in lattice QCD. I then describe recent advances aimed at extracting the momentum-dependent phase shifts from lattice calculations, notably in the meson sector, and the potential for their application to baryons. I conclude with a discussion of calculations of the electromagnetic transition form factors to excited nucleons, including calculations at high Q^2 .

Keywords Lattice QCD, spectroscopy, hadronic physics

1 Introduction

Lattice gauge theory provides a means of *solving* QCD in the low-energy regime, and thereby has a key role in hadronic and nuclear physics. The calculation of the low-lying spectrum, the masses of hadrons stable under the strong interactions, has long been a benchmark calculation for lattice QCD since it provides a confrontation between lattice QCD and precisely determined quantities in experiment. Such calculations are demanding, since they require a high degree of control over the systematic uncertainties inherent to lattice calculations, namely those arising from the finite volume in which they are performed, non-zero lattice spacing, and, finally, the need until recently to extrapolate from unphysical u and d quark masses to the physical light quark masses.

The focus of this talk is the spectrum of excited-state nucleons, and on the determination of their properties and photoproduction mechanisms. In fact, my emphasis will very much be on the former since it is a prerequisite for the latter; we will hear elsewhere in this workshop of recent theoretical developments aimed at a rigorous determination of hadronic matrix elements that involve multi-hadron states[16]. I will begin by reminding us briefly of the formalism of lattice QCD, and note some of the computational challenges. I will point out some recent successes at looking at the properties of stable hadrons such as the nucleon, before proceeding to describe how the spectrum of excited states can be determined on the lattice. In particular, I will focus on the use of the variational method, and how that can provide important insights both into the masses of their states, and their quark and gluon structure. I will then describe how resonances are treated in a lattice calculation, and the determination of the momentum-dependent phase shifts. I will conclude with a discussion of lattice calculations of transition form factors, and a summary.

Jefferson Lab
12000 Jefferson Avenue
Newport News, VA 23606
USA
Tel.: +1-757-269-7736
E-mail: dgr@jlab.org

2 Lattice QCD and the Properties of Ground-state Hadrons

Lattice QCD is Quantum Chromodynamics formulated on a Euclidean space-time lattice, with the “lattice spacing” fulfilling the rôle of a hard, ultraviolet cut-off. An “observable” in lattice QCD can be calculated through the evaluation of the discretized path integral

$$\langle \mathcal{O} \rangle = \frac{1}{Z} \prod_{x,\mu} dU_\mu(x) \prod_x d\psi(x) \prod_x d\bar{\psi}(x) \mathcal{O}(U, \psi, \bar{\psi}) e^{-S(U, \psi, \bar{\psi})}, \quad (1)$$

where $U_\mu(x)$ are $SU(3)$ matrices representing the gluonic degrees of freedom, and $\psi, \bar{\psi}$ are Grassmann variables representing the quarks. Writing the QCD action in terms of the pure gauge and fermion components, we have

$$S(U, \psi, \bar{\psi}) = S_g(U) + \bar{\psi} M(U) \psi,$$

whence we can integrate the fermion degrees of freedom to yield

$$\langle \mathcal{O} \rangle = \frac{1}{Z} \prod_{x,\mu} dU_\mu(x) \mathcal{O}(U) \det M(U) e^{-S_g(U)}. \quad (2)$$

The need to formulate the theory in Euclidean space is now clear: eqn 2 can be estimated using the *importance sampling* methods familiar to statistical physics, since the action $S_g(U)$, and indeed the determinant, are real. A lattice gauge calculation therefore consists, firstly, of generating an ensemble of equilibrated gauge configuration $\{U_\mu^n(x) : n = 1, \dots, N_{\text{cfg}}\}$ distributed according to

$$P(U) \propto \det M(U) e^{-S_g(U)} \quad (3)$$

and then calculating the expectation value of the operator \mathcal{O} on

$$\langle \mathcal{O} \rangle = \frac{1}{N_{\text{cfg}}} \sum_{n=1}^{N_{\text{cfg}}} \mathcal{O}(U^n, G[U^n]) \quad (4)$$

where $G[U^n]$ represent quark propagators computed on the gauge field $U_\mu^n(x)$. The generation of the gauge fields in eqn 3 is a *capability* computing task in which the whole, or at least a sizable proportion, of a leadership-class computer has to be devoted to a single sequence of Monte Carlo calculations to yield a thermalized distribution. The evaluation of $\det M(U)$ is dominant, since any local change to gauge links $U_\mu(x)$ requires the evaluation of the determinant over the whole lattice, in contrast to a pure-gauge calculation where the change in $S_g(U)$ can be evaluated locally. The evaluation of eqn 4 is inherently a *capacity* computing task, since the calculation of $\mathcal{O}(U^n)$ can be performed on each configuration independently. For many of the calculations described below, the integrated cost of these computations can far exceed those of eqn 3, but these can exploit cost-optimized clusters and GPU-accelerated clusters.

The spectrum of QCD is determined through the exponential decay of two-point correlation functions

$$C(t) = \sum_{\mathbf{x}} \langle 0 | \mathcal{O}(\mathbf{x}, t) \bar{\mathcal{O}}(0) | 0 \rangle \longrightarrow \sum_n A_n e^{-E_n t}, \quad (5)$$

where \mathcal{O} is an interpolating operator, say for the nucleon, and the E_n and A_n are the energies and residues of all states n with $\langle n | \bar{\mathcal{O}} | 0 \rangle \neq 0$; the energies E_n are real, reflecting the formulation in Euclidean space. The masses of the low-lying states of the spectrum, that is states stable under the strong interaction, are determined from the leading exponential in eqn 5.

As noted earlier, calculations that can directly confront experiment require control over a variety of systematic uncertainties. A prominent example of such a calculation, for states composed of the u, d and s quarks, was that of the BMW collaboration[31], and they have recently extended their work through the inclusion of QED computations to provide a calculation of the proton-neutron mass difference, as well as that for other hadrons[13]. Beyond the low-lying spectrum, calculations are also being performed of the matrix elements of the nucleon, including those for the (space-like) electric and magnetic form factors, and for the moments of parton distributions and Generalized Parton Distributions, initially for the isovector properties, but now extended to include the effects of the sea quarks; for a recent review,

see ref. [26]. For each of these quantities, calculations in Euclidean space can be directly related to quantities in Minkowski space. None-the-less, even for ground-state hadrons, there are limitations to properties that can be straightforwardly calculated, notably the matrix elements of the quark bilinears separated along the light cone that give rise to the (generalized) parton distribution functions and transverse-momentum-dependent distributions, and methods have been proposed[37; 55; 45] and indeed applied, to circumvent these issues in Euclidean-space calculations.

3 The excited-state spectrum in lattice QCD

The first challenge in the study of the excited-state spectrum is to effectively determine the subleading exponentials in eqn 5. A robust way of doing so is by means of the variational method, whereby we compute a matrix of correlation functions

$$C_{ij}(t) = \sum_{\mathbf{x}} \langle 0 | \mathcal{O}_i^{J^P}(\mathbf{x}, t) \bar{\mathcal{O}}_j^{J^P}(\mathbf{0}, 0) | 0 \rangle \longrightarrow \sum_n A_{ij}^n e^{-E_n t}, \quad (6)$$

where $\{\mathcal{O}_i^{J^P} : i = 1, \dots, N\}$ is a basis of operators, each having common quantum numbers. We now solve the generalized eigenvalue equation

$$C(t)u(t, t_0) = \lambda(t, t_0)C(t_0)u(t, t_0) \quad (7)$$

yielding a set of real eigenvalues $\{\lambda_n(t, t_0) : n = 1, \dots, N\}$ with corresponding eigenvectors $\{u^n(t, t_0) : n = 1, \dots, N\}$, where, for sufficiently large t , we have $\lambda_0 \geq \lambda_1 \geq \dots$. These delineate the different states

$$\lambda_n(t, t_0) \rightarrow (1 - A)e^{-E_n(t-t_0)} + Ae^{-(E_n + \Delta E_n)(t-t_0)}. \quad (8)$$

The application of the variational method relies on the construction of a suitable basis of interpolating operators. In the case of the nucleon, there are only three local interpolating operators that can be constructed from three quark fields, such that at most three energies can be determined:

$$\mathcal{O}^{1/2} = \begin{cases} (uC\gamma_5 d)u \\ (uCd)\gamma_5 u \\ (uC\gamma_4\gamma_5 d)u \end{cases}. \quad (9)$$

The basis of operators can be extended to include quasi-local quark operators through the use of gauge-invariant smearing whereby a quark field $\psi(\mathbf{x}, t) \rightarrow \bar{\psi}(\mathbf{x}, t) = \sum_{\mathbf{y}} L(\mathbf{x}, \mathbf{y})\psi(\mathbf{y})$ where $L(\mathbf{x}, \mathbf{y})$ is a gauge-covariant operator, such as the inverse of a three-dimensional Laplacian; such a construction does not alter the angular-momentum structure of a nucleon operator. There have been many studies in the last few years that have aimed at extracting the excited-state nucleon spectrum of both parities through the use of the variational method[7; 24; 25; 46; 48; 47; 49], as well as through techniques such as the sequential-Bayes method aimed at delineating subleading terms from only a single correlator[50]. A basis of operators with different smearing radii for the quark fields can capture the radial structure of the nucleons, and indeed allow for nodes in the wave function. However, it appears incomplete in that it does not capture the orbital structure. To do so, and indeed to study states of spin higher than 3/2, requires operators that are non-local, either by displacing one or more of the quarks, or equivalently, through the use of covariant derivatives acting on the quark fields. Such constructions, in which the bases of operators were designed in the first instance to satisfy the symmetries of the lattice, were introduced in refs. [10] and [11], and applied in refs. [12; 23; 22], providing, for the first time, access to states of spin 5/2 and higher.

The lack of rotational symmetry introduced through the discretisation onto a finite space-time lattice has the consequence that angular momentum is no longer a good quantum number at any finite spacing. We find in the meson sector that a remarkable degree of rotational symmetry in operator overlaps is realized at the hadronic scale, enabling the ‘‘single-particle’’ spectrum to be classified according to the total angular momentum of the states[28; 29]. We exploit this observation in constructing a

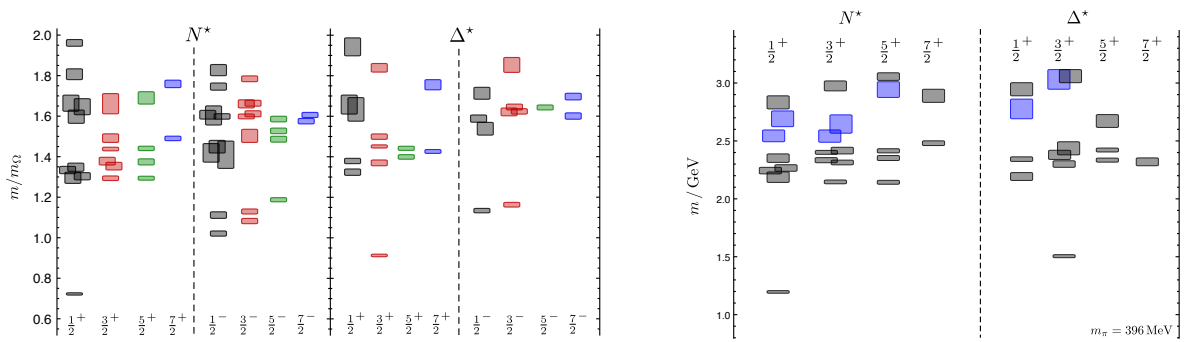


Fig. 1 The left-hand plot shows the spin-identified excited nucleon and Δ spectra in units of the Ω mass obtained on a $16^3 \times 64$ anisotropic clover lattice with the strange quark mass at its physical value, and the light-quark masses corresponding to a pion mass of 396 MeV[32]. The right-hand plot shows the positive-parity spectrum for both the nucleon and Δ in physical units using an operator basis with the “hybrid” operators included[27]. The additional states that couple predominantly to the hybrid-type operators are shown in blue.

basis of interpolating operators for baryons. We begin by expressing continuum baryon interpolating operators of definite J^P as[32; 33]

$$\mathcal{O}^{J^P} \sim \left(F_{\Sigma_F} \otimes (S^{P_s})_{\Sigma_S}^n \otimes D_{L, \Sigma_D}^{[d]} \right)^{J^P}, \quad (10)$$

where F , S and D are the flavor, Dirac spin and orbital angular momentum parts of the wave function, and the Σ 's express the corresponding permutation symmetry: Symmetric (S), mixed-symmetric (MS), mixed anti-symmetric (MA), and anti-symmetric (A).

Non-zero orbital angular momentum is introduced through the use of gauge-covariant derivatives, written in a circular basis and acting on the quark fields. In the notation above, $D_{L, \Sigma_D}^{[d]}$ corresponds to an orbital wave function constructed from d derivatives, and projected onto orbital angular momentum L . In the calculations described here, up to two covariant derivatives are employed, enabling orbital angular momentum up to $L = 2$ to be accessed, and therefore states up to spin $7/2$ to be studied; the spin-identified spectrum obtained using such a basis of operators is shown as the left-hand plot in Figure 1. The spectrum reveals a counting consistent with that of a qqq non-relativistic quark model, and richer than certain quark-diquark pictures.

A faithful extraction of the spectrum is contingent on having a sufficiently complete basis of operators. In the analysis described above, one particular operator is absent, namely the mixed-symmetric combination $D_{L=1, M}^{[2]}$, the commutator of two covariant derivatives projected to $L = 1$, that corresponds to a chromo-magnetic field that would vanish for trivial gauge field configuration; operators with this construction we identify as *hybrid* operators, associated with a manifest gluon content[27]. The right-hand plot of Figure 1 is the positive-parity nucleon and Δ spectrum on the same ensemble as that used in the left-hand plot, showing the additional states appearing when this more complete basis of operators is employed. The conclusion is that, with the addition of these operators, the counting of states is still richer than the quark model, with the additional states attributable to a coupling to a colour-octet gluonic excitation.

One feature of the experimentally observed nucleon spectrum that is absent in Figure 1 is a low-lying Roper resonance, a positive-parity excitation *below* the lowest-lying negative-parity state. This feature of a quark-model type ordering of the low-lying positive- and negative-parity excitations is a feature of most of the lattice calculations discussed above. The exception to this is the calculation of the χ QCD group, using overlap fermions on an ensemble generated using domain-wall fermions[42]; their calculation, together with the results of other groups, is shown in Figure 2. It has been argued that the lattice calculations of the Roper are incomplete, lacking the multi-hadron operators as we discuss below, but not inconsistent with the observed spectrum[39].

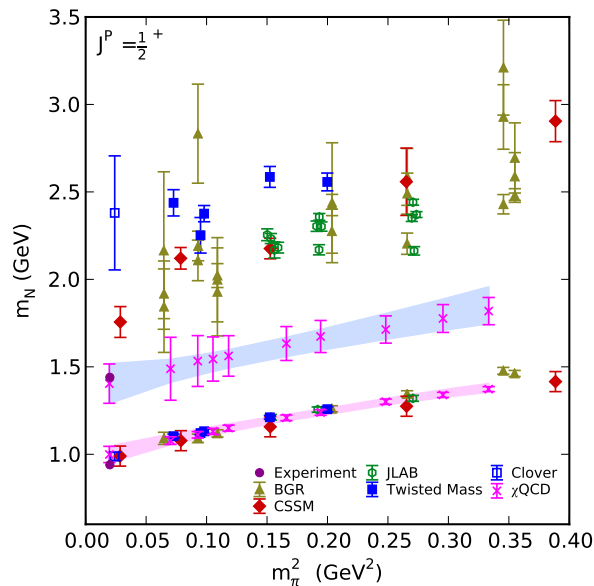


Fig. 2 Calculations of the lowest-lying positive parity excitation of the nucleon, taken from reference [42]. The χ QCD results are obtained using overlap fermions on an ensemble generated using domain-wall fermions.

3.1 Multi-hadron Spectrum and the nature of resonances

Lattice QCD is formulated in Euclidean space, and the energies entering into the spectral decomposition of eqn. 6 are real. On a finite, discretized Euclidean lattice, the spatial momenta are quantized, and the calculated discrete spectrum, that is the energies of eqn 5, should include two- and higher-body scattering states. Indeed, even at the unphysically large quark masses used in Figure 1, many of the higher excitations are above decay thresholds. For non-interacting particles, the energies are given by the symmetries of the volume in which we are working and the allowed spatial momenta. The finite, periodic spatial volume forces those hadrons to interact thereby shifting the energies from their non-interacting values. For the case of elastic scattering, the so-called Lüscher method enables the shift in energies at a finite volume to be related to the infinite volume phase shift[43; 44], shortly thereafter extended to states with non-zero total momentum[52]. In the meson sector, the precise calculation of the momentum-dependent phase shifts for states such as the ρ meson in $I = 1 \pi\pi$ scattering has now been accomplished[30], and the formalism has been extended to the extraction of the momentum-dependent amplitudes for inelastic scattering[36; 34; 35; 17].

Analogous calculations in the baryon sector are less advanced. For most of the calculations discussed above, the interpolating operators were constructed from three quarks, albeit with quite elaborate orbital structures. The two-hadron energy levels that should be seen in the spectrum are in general absent, and their non-observation is attributed to the volume suppression of single-hadron operators to multi-hadron states. Several groups have included multi-hadron or five-quark operators in their basis[38; 54]. Notably, one group has included interpolators of the form $\mathcal{O}_{N\pi}(\mathbf{p}) = N^i(\mathbf{p})\pi(\mathbf{0})$, where $N^i, i = 1, 2, 3$, are the three local interpolators of eqn. 9, and observe $N\pi$ states as expected, but also the presence of an additional energy level in the spectrum. A different approach, applicable to transitions near threshold[51], has been applied to the decays of decuplet baryon resonances to an octet baryon-pion final state[5; 6]. However, the application of the full panoply of the Lüscher method is currently limited.

4 Electromagnetic transitions in N^* resonances

The formalism to extract infinite-volume transition matrix elements between states containing two or more hadrons from Euclidean space lattice calculations has only recently been developed[21; 19; 20], and applied to meson transitions[18]; it will be presented workshop[16]. Instead, I will backtrack somewhat

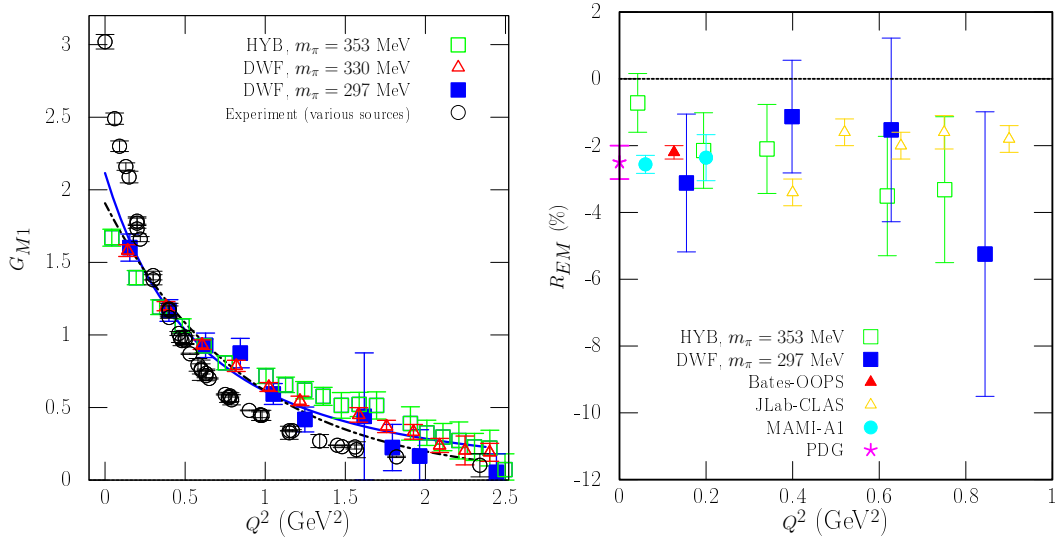


Fig. 3 The left-hand plot, taken from ref. [4] shows the magnetic dipole form factor $G_{M1}(Q^2)$ for the N to Δ transition. The right-hand plot, taken from the same paper, shows the ratio $R_{EM} = -G_{E2}(Q^2)/G_{M1}(Q^2)$.

and talk about calculations of electromagnetic properties in which both the incoming and outgoing particles are treated as single-particle states.

Hadronic matrix elements in lattice QCD are computed through the calculation of three-point functions:

$$\begin{aligned}
 C_{3\text{pt}}(t_f, t; \mathbf{p}, \mathbf{q}) &= \sum_{\mathbf{x}} \sum_{\mathbf{y}} \langle 0 | \mathcal{O}_1(\mathbf{x}, t_f) J(\mathbf{y}, t) \bar{\mathcal{O}}_2(0) | 0 \rangle e^{-i\mathbf{p}\cdot\mathbf{x}} e^{-i\mathbf{q}\cdot\mathbf{y}} \\
 &\rightarrow \langle 0 | \mathcal{O}_1 | N_1, \mathbf{p} \rangle \langle N_1, \mathbf{p} | \bar{\mathcal{O}}_2 | 0 \rangle \langle N_1, \mathbf{p} | J | N_2, \mathbf{p} + \mathbf{q} \rangle \\
 &\quad \times e^{-E_1(\mathbf{p})(t_f-t)} e^{-E_2(\mathbf{p}+\mathbf{q})t},
 \end{aligned} \tag{11}$$

with $Q^2 = (E_2(\mathbf{p}) - E_2(\mathbf{p} + \mathbf{q}))^2 - \mathbf{q}^2$, and where we treat \mathcal{O}_1 and \mathcal{O}_2 as ideal interpolating operators for the incoming and outgoing states, obtained, for example, from the eigenvectors obtained in the variational method[53].

The most widely studied transition is that to the Δ resonance[3; 4], though there was an earlier investigation of the P_{11} Roper transition[40]. The former is of particular interest both because there has been considerable experimental effort, and because a non-zero quadrupole moment can provide important information about the structure nucleon inaccessible from the proton form factor. A recent example of such a calculation is shown in Figure 3, for both the magnetic dipole transition form factor and for the ratio of the quadrupole to dipole form factors. As noted earlier, it must be emphasised that the interpretation of infinite-volume matrix elements for multi-hadron states requires considerable theoretical work[1; 2], and the application is computationally demanding.

As the momenta in eqn 11 increase, lattice calculations of the form factors become increasingly demanding, both because of decreasing signal-to-noise ratios and because of increasing discretisation errors. There have been several ideas that aim to overcome these issues[41; 8] to enable the direct calculation of the Q^2 dependence of the form factor, but another approach, applicable to hard, exclusive processes, is through the calculation of the hadronic wave functions for both the nucleon and for its excitations[9; 15]; that approach is described elsewhere at this workshop[14].

5 Summary

There has been far-reaching theoretical and computational progress aimed at understanding the excited state spectrum of QCD through lattice calculations. Much of the computational work has been centered on the meson sector, where the computational are considerably reduced. However, with the increasing

computational resources, and our increasing theoretical understanding, these ideas will be applied to the N^* spectrum, enabling lattice calculations to truly confront experiment.

Acknowledgements The author would like to thank his colleagues in the *HadSpec Collaboration* for discussions and collaboration on some of the work. I am grateful to the authors of refs. [42] and [4] for use of their figures. This material is based upon work supported by the U.S. Department of Energy, Office of Science, Office of Nuclear Physics under contract DE-AC05-06OR23177.

References

1. Agadjanov A, Bernard V, Meißner UG, Rusetsky A (2014) A framework for the calculation of the $N\Delta\gamma^*$ transition form factors on the lattice. Nucl Phys B886:1199–1222, DOI 10.1016/j.nuclphysb.2014.07.023, 1405.3476
2. Agadjanov A, Bernard V, Meißner UG, Rusetsky A (2016) Resonance matrix elements on the lattice. EPJ Web Conf 112:01,001, DOI 10.1051/epjconf/201611201001
3. Alexandrou C, Leontiou T, Negele JW, Tsapalis A (2007) The Axial N to Delta transition form factors from Lattice QCD. Phys Rev Lett 98:052,003, DOI 10.1103/PhysRevLett.98.052003, hep-lat/0607030
4. Alexandrou C, Koutsou G, Negele JW, Proestos Y, Tsapalis A (2011) Nucleon to Delta transition form factors with $N_F = 2 + 1$ domain wall fermions. Phys Rev D83:014,501, DOI 10.1103/PhysRevD.83.014501, 1011.3233
5. Alexandrou C, Negele JW, Petschlies M, Pochinsky AV, Syritsyn SN (2015) Study of decuplet baryon resonances from lattice QCD 1507.02724
6. Alexandrou C, Negele JW, Petschlies M, Pochinsky AV, Syritsyn SS (2015) Calculation of the decay width of decuplet baryons. In: Proceedings, 33rd International Symposium on Lattice Field Theory (Lattice 2015), URL <https://inspirehep.net/record/1403565/files/arXiv:1511.02752.pdf>, 1511.02752
7. Allton CR, et al (1993) Gauge invariant smearing and matrix correlators using Wilson fermions at Beta = 6.2. Phys Rev D47:5128–5137, DOI 10.1103/PhysRevD.47.5128, hep-lat/9303009
8. Bali GS, Lang B, Musch BU, Schäfer A (2016) A novel quark smearing for hadrons with high momenta in lattice QCD 1602.05525
9. Bali GS, et al (2016) Light-cone distribution amplitudes of the baryon octet. JHEP 02:070, DOI 10.1007/JHEP02(2016)070, 1512.02050
10. Basak S, Edwards R, Fleming GT, Heller UM, Morningstar C, Richards D, Sato I, Wallace SJ (2005) Clebsch-Gordan construction of lattice interpolating fields for excited baryons. Phys Rev D72:074,501, DOI 10.1103/PhysRevD.72.074501, hep-lat/0508018
11. Basak S, Edwards RG, Fleming GT, Heller UM, Morningstar C, Richards D, Sato I, Wallace S (2005) Group-theoretical construction of extended baryon operators in lattice QCD. Phys Rev D72:094,506, DOI 10.1103/PhysRevD.72.094506, hep-lat/0506029
12. Basak S, Edwards RG, Fleming GT, Juge KJ, Lichtl A, Morningstar C, Richards DG, Sato I, Wallace SJ (2007) Lattice QCD determination of patterns of excited baryon states. Phys Rev D76:074,504, DOI 10.1103/PhysRevD.76.074504, 0709.0008
13. Borsanyi S, et al (2015) Ab initio calculation of the neutron-proton mass difference. Science 347:1452–1455, DOI 10.1126/science.1257050, 1406.4088
14. Braun V (2016) these proceedings
15. Braun VM, Collins S, Gläbke B, Göckeler M, Schäfer A, Schiel RW, Söldner W, Sternbeck A, Wein P (2014) Light-cone Distribution Amplitudes of the Nucleon and Negative Parity Nucleon Resonances from Lattice QCD. Phys Rev D89:094,511, DOI 10.1103/PhysRevD.89.094511, 1403.4189
16. Briceño R (2016) these proceedings
17. Briceño RA, Davoudi Z (2013) Moving multichannel systems in a finite volume with application to proton-proton fusion. Phys Rev D88(9):094,507, DOI 10.1103/PhysRevD.88.094507, 1204.1110
18. Briceño RA, Dudek JJ, Edwards RG, Shultz CJ, Thomas CE, Wilson DJ (2015) The resonant $\pi^+\gamma \rightarrow \pi^+\pi^0$ amplitude from Quantum Chromodynamics. Phys Rev Lett 115:242,001, DOI 10.1103/PhysRevLett.115.242001, 1507.06622
19. Briceño RA, Hansen MT (2015) Multichannel $0 \rightarrow 2$ and $1 \rightarrow 2$ transition amplitudes for arbitrary spin particles in a finite volume. Phys Rev D92(7):074,509, DOI 10.1103/PhysRevD.92.074509, 1502.04314
20. Briceño RA, Hansen MT (2015) Relativistic, model-independent, multichannel $2 \rightarrow 2$ transition amplitudes in a finite volume 1509.08507
21. Briceño RA, Hansen MT, Walker-Loud A (2015) Multichannel $1 \rightarrow 2$ transition amplitudes in a finite volume. Phys Rev D91(3):034,501, DOI 10.1103/PhysRevD.91.034501, 1406.5965
22. Bulava J, Edwards RG, Engelson E, Joo B, Lin HW, Morningstar C, Richards DG, Wallace SJ (2010) Nucleon, Δ and Ω excited states in $N_f = 2 + 1$ lattice QCD. Phys Rev D82:014,507, DOI 10.1103/PhysRevD.82.014507, 1004.5072
23. Bulava JM, et al (2009) Excited State Nucleon Spectrum with Two Flavors of Dynamical Fermions. Phys Rev D79:034,505, DOI 10.1103/PhysRevD.79.034505, 0901.0027
24. Burch T, Gatttringer C, Glozman LYa, Kleindl R, Lang CB, Schaefer A (2004) Spatially improved operators for excited hadrons on the lattice. Phys Rev D70:054,502, DOI 10.1103/PhysRevD.70.054502, hep-lat/0405006

-
25. Burch T, Gatttringer C, Glozman LYa, Hagen C, Lang CB, Schafer A (2006) Excited hadrons on the lattice: Mesons. *Phys Rev D* 73:094,505, DOI 10.1103/PhysRevD.73.094505, [hep-lat/0601026](#)
 26. Constantinou M (2015) Recent progress in hadron structure from Lattice QCD. In: 8th International Workshop on Chiral Dynamics (CD 2015) Pisa, Italy, June 29-July 3, 2015, URL <https://inspirehep.net/record/1402363/files/arXiv:1511.00214.pdf>, 1511.00214
 27. Dudek JJ, Edwards RG (2012) Hybrid Baryons in QCD. *Phys Rev D* 85:054,016, DOI 10.1103/PhysRevD.85.054016, 1201.2349
 28. Dudek JJ, Edwards RG, Peardon MJ, Richards DG, Thomas CE (2009) Highly excited and exotic meson spectrum from dynamical lattice QCD. *Phys Rev Lett* 103:262,001, DOI 10.1103/PhysRevLett.103.262001, 0909.0200
 29. Dudek JJ, Edwards RG, Peardon MJ, Richards DG, Thomas CE (2010) Toward the excited meson spectrum of dynamical QCD. *Phys Rev D* 82:034,508, DOI 10.1103/PhysRevD.82.034508, 1004.4930
 30. Dudek JJ, Edwards RG, Thomas CE (2013) Energy dependence of the ρ resonance in $\pi\pi$ elastic scattering from lattice QCD. *Phys Rev D* 87(3):034,505, DOI 10.1103/PhysRevD.87.034505, 10.1103/PhysRevD.90.099902, [Erratum: *Phys. Rev. D* 90, no. 9, 099902 (2014)], 1212.0830
 31. Durr S, et al (2008) Ab-Initio Determination of Light Hadron Masses. *Science* 322:1224–1227, DOI 10.1126/science.1163233, 0906.3599
 32. Edwards RG, Dudek JJ, Richards DG, Wallace SJ (2011) Excited state baryon spectroscopy from lattice QCD. *Phys Rev D* 84:074,508, DOI 10.1103/PhysRevD.84.074508, 1104.5152
 33. Edwards RG, Mathur N, Richards DG, Wallace SJ (2013) Flavor structure of the excited baryon spectra from lattice QCD. *Phys Rev D* 87(5):054,506, DOI 10.1103/PhysRevD.87.054506, 1212.5236
 34. Guo P, Dudek J, Edwards R, Szczepaniak AP (2013) Coupled-channel scattering on a torus. *Phys Rev D* 88(1):014,501, DOI 10.1103/PhysRevD.88.014501, 1211.0929
 35. Hansen MT, Sharpe SR (2012) Multiple-channel generalization of Lellouch-Luscher formula. *Phys Rev D* 86:016,007, DOI 10.1103/PhysRevD.86.016007, 1204.0826
 36. He S, Feng X, Liu C (2005) Two particle states and the S-matrix elements in multi-channel scattering. *JHEP* 07:011, DOI 10.1088/1126-6708/2005/07/011, [hep-lat/0504019](#)
 37. Ji X (2013) Parton Physics on a Euclidean Lattice. *Phys Rev Lett* 110:262,002, DOI 10.1103/PhysRevLett.110.262002, 1305.1539
 38. Kiratidis AL, Kamleh W, Leinweber DB, Owen BJ (2015) Lattice baryon spectroscopy with multi-particle interpolators. *Phys Rev D* 91:094,509, DOI 10.1103/PhysRevD.91.094509, 1501.07667
 39. Leinweber D, Kamleh W, Kiratidis A, Liu ZW, Mahbub S, Roberts D, Stokes F, Thomas AW, Wu J (2015) N^* Spectroscopy from Lattice QCD: The Roper Explained. In: 10th International Workshop on the Physics of Excited Nucleons (NSTAR 2015) Osaka, Japan, May 25-28, 2015, URL <https://inspirehep.net/record/1407159/files/arXiv:1511.09146.pdf>, 1511.09146
 40. Lin HW, Cohen SD, Edwards RG, Richards DG (2008) First Lattice Study of the $N - P(11)(1440)$ Transition Form Factors. *Phys Rev D* 78:114,508, DOI 10.1103/PhysRevD.78.114508, 0803.3020
 41. Lin HW, Cohen SD, Edwards RG, Orginos K, Richards DG (2010) Lattice Calculations of Nucleon Electromagnetic Form Factors at Large Momentum Transfer 1005.0799
 42. Liu KF, Chen Y, Gong M, Sufian R, Sun M, Li A (2014) The Roper Puzzle. *PoS LATTICE2013*:507, 1403.6847
 43. Luscher M (1986) Volume Dependence of the Energy Spectrum in Massive Quantum Field Theories. 2. Scattering States. *Commun Math Phys* 105:153–188, DOI 10.1007/BF01211097
 44. Luscher M (1991) Two particle states on a torus and their relation to the scattering matrix. *Nucl Phys B* 354:531–578, DOI 10.1016/0550-3213(91)90366-6
 45. Ma YQ, Qiu JW (2014) Extracting Parton Distribution Functions from Lattice QCD Calculations 1404.6860
 46. Mahbub MS, O Cais A, Kamleh W, Lasscock BG, Leinweber DB, Williams AG (2009) Isolating Excited States of the Nucleon in Lattice QCD. *Phys Rev D* 80:054,507, DOI 10.1103/PhysRevD.80.054507, 0905.3616
 47. Mahbub MS, Kamleh W, Leinweber DB, O Cais A, Williams AG (2010) Ordering of Spin- $\frac{1}{2}$ Excitations of the Nucleon in Lattice QCD. *Phys Lett B* 693:351–357, DOI 10.1016/j.physletb.2010.08.049, 1007.4871
 48. Mahbub MS, Kamleh W, Leinweber DB, Moran PJ, Williams AG (2012) Roper Resonance in 2+1 Flavor QCD. *Phys Lett B* 707:389–393, DOI 10.1016/j.physletb.2011.12.048, 1011.5724
 49. Mahbub MS, Kamleh W, Leinweber DB, Moran PJ, Williams AG (2013) Low-lying Odd-parity States of the Nucleon in Lattice QCD. *Phys Rev D* 87(1):011,501, DOI 10.1103/PhysRevD.87.011501, 1209.0240
 50. Mathur N, Chen Y, Dong SJ, Draper T, Horvath I, Lee FX, Liu KF, Zhang JB (2005) Roper resonance and $S(11)(1535)$ from lattice QCD. *Phys Lett B* 605:137–143, DOI 10.1016/j.physletb.2004.11.010, [hep-ph/0306199](#)
 51. McNeile C, Michael C (2003) Hadronic decay of a vector meson from the lattice. *Phys Lett B* 556:177–184, DOI 10.1016/S0370-2693(03)00130-8, [hep-lat/0212020](#)
 52. Rummukainen K, Gottlieb SA (1995) Resonance scattering phase shifts on a nonrest frame lattice. *Nucl Phys B* 450:397–436, DOI 10.1016/0550-3213(95)00313-H, [hep-lat/9503028](#)
 53. Shultz CJ, Dudek JJ, Edwards RG (2015) Excited meson radiative transitions from lattice QCD using variationally optimized operators. *Phys Rev D* 91(11):114,501, DOI 10.1103/PhysRevD.91.114501, 1501.07457
 54. Verduci V, Lang CB (2014) Baryon resonances coupled to Pion-Nucleon states in lattice QCD. *PoS LATTICE2014*:121, 1412.0701

-
55. Xiong X, Ji X, Zhang JH, Zhao Y (2014) One-loop matching for parton distributions: Nonsinglet case. *Phys Rev D* 90(1):014,051, DOI 10.1103/PhysRevD.90.014051, 1310.7471